

High order finite elements

Sílvia Barbeiro

CMUC, Departamento de Matemática, Universidade de Coimbra, e-mail: `silvia@mat.uc.pt`

1 Introduction

The great advances in computational mathematics over the last half century, driven by profound developments in numerical methods along with remarkable progresses in the field of high performance computing, are playing a major role in the scientific and engineering innovation.

Partial differential equations arise in the mathematical modelling of many physical, chemical and biological phenomena in a wide and diverse range of subject areas such as fluid dynamics, electromagnetism, material science, medical imaging. Very frequently is either impossible or impracticable to find closed form solutions to the equations under consideration and it is crucial to obtain numerical approximations to the unknown analytical solution.

When assigned with the task of solving numerically a partial differential equation, the first question one faces is to choose an adequate method.

The demand for finding accurate numerical models for physical phenomena around complex geometries are making high order methods very attractive for practical applications. Among the possible choices, the discontinuous Galerkin (DG) finite element method, which ensures geometric flexibility and supports high order locally adapted resolution, appears to offer most of the desired properties.

The DG finite element method appeared in the literature back to 1973 in [16], as a proposal to solve the steady-state neutron transport equation. The first convergence analysis results were presented in 1974, in [13] and improved later for example in [12], [14] and [15]. The extension to nonlinear scalar conservation laws was achieved in late 1980's ([4]). Important progresses, namely the development of adaptive solution techniques and the extension to multidimensional cases and to unstructured grids, took place in the next two decades (see *e.g.* [5], [11]). Since the years 2000 there has been an explosion in activities and DG methods become widely used for solving a large range of problems, for example, electromagnetic wave's propagation ([8]), or fluid flow in porous media ([17]).

Being capable of producing highly accurate numerical solutions, DG methods gather many desirable features over the finite differences, finite volume and finite element methods, when used to derive spacial discretizations. The widely used finite differences, on top of being simple, lead to very efficient schemes in many problems. However they are not suitable to handle complex geometries. The finite volume method, uses an element based approach and ensures geometric flexibility. Moreover it is locally conservative. The main drawback of the finite volume method is its limitation for achieve high-order accuracy on general unstructured grids. The need to solve geometrically complex large scale problems with higher-order convergence, justifies the huge interest in the flexibility offered by the finite element schemes, which is the natural choice in many problems. However, the basis functions are globally defined and consequently it is not straightforward to deal for instance with hanging nodes. While the mass matrix is sparse and typically well conditioned, finding, for instance, a steady state solution implies to solve a system that involves the global mass matrix. In addition, the finite element method is less natural when compared with finite volume method to deal with conservation laws, where there is a flow in specific directions. Discontinuous Galerkin methods fulfill the need of geometrical flexibility and locally adapted resolution. Some other features include local mass conservation, possible definition on unstructured meshes, *hp*-adaptivity with locally varying polynomial degrees.

There is likewise a wide variety of methods for the integration in time. For example, we can mention the fully explicit leap-frog method ([1]), or the classes of implicit and explicit Runge-Kutta type methods (*e.g.* [3],[10]), which reflect a method-of-lines approach with the time and space separately discretized. Explicit time-stepping schemes are computationally very effective. Nevertheless, those methods are only conditionally stable. If an explicit time integrator is considered, the maximum time step size allowed is related with the smallest elements of the spatial mesh. Locally refined meshes often obstruct the efficiency for the simulation of time-dependent phenomena, because of the stringent stability constraint caused by the existence of some small elements in the

spatial mesh. This could be the case when the problem involves modelling small structures with complex shapes and consequently a very fine mesh is needed at some spatial locations. As an example we mention the use of Maxwell's equation to model the electromagnetic wave's propagation in the human retina described in [2] and [18]. Simulating the full complexity of the retina, in particular taking into account the variation of the size and shape of each structure, demands the use of a spatial mesh which reflects that level of detail. This is remarkably limitative for the choice of the time step in the case of explicit time-stepping schemes.

By taking smaller time-steps precisely where the smallest elements are located, local time-stepping methods ([9]) become a possible approach. Another interesting choice, is to consider locally implicit time-schemes ([6]). Here we highlight another alternative, which is to consider the DG method in time. In contrast to explicit Runge-Kutta methods, the DG in time is unconditionally stable ([7]). This idea suggests the use of DG methods in a space-time approach, giving a framework for high-order accurate methods. In this technique, time is considered as an extra dimension and it is treated in a similar fashion as the spatial coordinates.

The advantages of DG methods include their flexibility on the choice of meshes and thus their capacity to handle complicated geometries, their potential for error control and mesh adaptation, their possible definition on unstructured meshes. The possibility of parallel implementation attenuates the major drawbacks which are high memory requirements and computational cost.

In spite of the theoretical developments, which encourage the use of high order finite element methods, the range of polynomial degrees used in finite element computations for practical applications and in commercial codes is usually rather small. In many cases, this fact is due to computational efficiency rather than any theoretical issue. The search of efficient solvers for the linear systems originated from the DG finite element approach is nowadays a trend of utmost importance.

In what follows we will briefly discuss the formulation of the DG finite element method for linear wave problems. We will also summarise the theoretical convergence properties to give an appreciation of what can be expected in terms of accuracy of the schemes.

2 The continuous setting

Let Ω be an open, bounded, Lipschitz domain in \mathbb{R}^d , $d \geq 1$, and let $T > 0$ be a finite time. We consider the following linear evolution problem: find $u : \Omega \times [0, T] \rightarrow \mathbb{R}$ such that

$$\begin{aligned} \frac{\partial u}{\partial t} + Au &= f \quad \text{in } \Omega \times (0, T], \\ u(\cdot, 0) &= u_0 \quad \text{in } \Omega, \\ u &= 0 \quad \text{on } \Gamma_- \times (0, T), \end{aligned} \quad (1)$$

where A is a first-order linear differential operator

$$Au = \beta \cdot \nabla u + \sigma u,$$

$\beta : \Omega \rightarrow \mathbb{R}^d$ is a given Lipschitz convection field, $\sigma : \Omega \rightarrow \mathbb{R}$ is a bounded reaction term, $f : \Omega \times [0, T] \rightarrow \mathbb{R}$ is the source term, $u_0 : \Omega \rightarrow \mathbb{R}$ is the initial datum, and Γ_- is the inflow part of the boundary defined as

$$\Gamma_- = \{x \in \Gamma : -\beta(x) \cdot n > 0\},$$

with n denoting the outer normal unit vector to Γ . The outflow boundary, Γ_+ , is defined by $\Gamma_+ = \Gamma \setminus \Gamma_-$. We make the following hypothesis on the data

$$\sigma(x) - \frac{1}{2} \operatorname{div} \beta(x) \geq \mu_0 > 0 \quad \forall x \in \Omega.$$

Let us consider the space

$$V = \{v \in L^2(\Omega) : \beta \cdot \nabla v \in L^2(\Omega), v|_{\Gamma_-} = 0\},$$

endowed with the norm

$$\|v\|_V^2 = \mu_0 \|v\|_{L^2(\Omega)}^2 + \|\beta \cdot \nabla v\|_{L^2(\Omega)}^2.$$

Assuming that $f \in C^0([0, T], L^2(\Omega))$ and $u_0 \in V$, taking the L^2 -inner product, from (1) we obtain the following variational problem: find $u \in C^0([0, T], V) \cap C^1([0, T], L^2(\Omega))$ such that, $\forall v \in L^2(\Omega)$, $\forall t \in (0, T]$,

$$\begin{aligned} \left(\frac{\partial u}{\partial t}(t), v \right)_{L^2(\Omega)} + (Au(t), v)_{L^2(\Omega)} &= (f(t), v)_{L^2(\Omega)} \\ u(0) &= u_0. \end{aligned} \quad (2)$$

Using the relation

$$\begin{aligned} (\beta \cdot \nabla u + \sigma u, u)_{L^2(\Omega)} &= (\sigma - \frac{1}{2} \operatorname{div} \beta, u^2)_{L^2(\Omega)} \\ &\quad + \frac{1}{2} ((\beta \cdot n)u, u)_{L^2(\Gamma)}, \end{aligned}$$

we can derive the following energy inequality, which expresses the continuous dependence of the solution of (2) on the data,

$$\begin{aligned} \|u(t)\|_{L^2(\Omega)}^2 + \int_0^t e^{t-\tau} \int_{\Gamma_+} (\beta(x) \cdot n(x)) u(x, \tau)^2 dx d\tau \\ \leq e^t \|u_0\|_{L^2(\Omega)}^2 + \int_0^t e^{t-\tau} \|u(\tau)\|_{L^2(\Omega)}^2 d\tau, \quad t \in [0, T]. \end{aligned}$$

The proof of the uniqueness of solution follows from the above inequality. Further results on the well-posedness of (2), namely the existence of solution, can be found in [19].

3 The discrete setting

We introduce some key ideas behind the DG finite element method in a simple case, considering the scalar wave equation

$$\frac{\partial u}{\partial t} + a \frac{\partial u}{\partial x} = 0, \quad x \in (0, 1) = \Omega, \quad t \in (0, T], \quad (3)$$

with $a > 0$, subject to the initial condition $u(x, 0) = u_0(x)$ and the inflow boundary condition $u(0, t) = 0$.

Assume that the computational domain Ω is partitioned into K nonoverlapping elements D_k such that

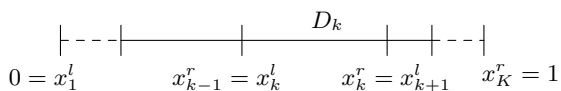


Fig. 1. Partition of the computational domain in 1 dimension.

$\bar{\Omega} = \cup_k D_k$, as illustrated in the Figure 1. On each element D_k , the solution is approximated by polynomials of degree less than or equal to $N = N_p - 1$,

$$\tilde{u}_k(x, t) = \sum_{n=1}^{N_p} \hat{u}_n^k(t) \varphi_n(x),$$

where φ_n , $n = 1, \dots, N_p$, form the local polynomial basis. The global solution $u(x, t)$ is then assumed to be approximated by the piecewise N order polynomials defined as the direct sum of the K local polynomial solutions

$$u(x, t) \simeq \tilde{u}(x, t) = \bigoplus_{k=1}^K \tilde{u}_k(x, t).$$

In order to deduce the method, we start by multiplying equation (3) by test functions φ_n . Spatial integration by parts over each element D_k yields

$$\begin{aligned} \int_{D_k} \left(\frac{\partial \tilde{u}_k}{\partial t} \varphi_n - a \tilde{u}_k \frac{\partial \varphi_n}{\partial x} \right) dx &= - \left[a \tilde{u}_k \varphi_n \right]_{x_k^l}^{x_k^r} \\ &= - \int_{\partial D_k} n \cdot a \tilde{u}_k \varphi_n dx, \quad 1 \leq n \leq N_p, \end{aligned}$$

where n represents the local outward pointing normal. The next step is to substitute in the resulting contour integral the flux by a numerical flux $(a\tilde{u})^*$, which will be specified later. Reversing the integration by parts yields

$$\begin{aligned} \int_{D_k} \left(\frac{\partial \tilde{u}_k}{\partial t} \varphi_n + a \frac{\partial \tilde{u}_k}{\partial x} \varphi_n \right) dx \\ = \int_{\partial D_k} n \cdot (a \tilde{u}_k - (a\tilde{u})^*) \varphi_n dx, \quad 1 \leq n \leq N_p. \end{aligned}$$

The approximate solution is allowed to be discontinuous across elements boundaries. In this way, we introduce the notation of average $\{\{\tilde{u}\}\} = \frac{\tilde{u}^- + \tilde{u}^+}{2}$ and of the jumps of the solution values across the interfaces of the elements, $[\tilde{u}] = \tilde{u}^- - \tilde{u}^+$, where the superscript “+” denotes the neighbouring element and the superscript “-” refers to the local element. The coupling between elements is introduced via the numerical flux

$$(a\tilde{u})^* = \{\{a\tilde{u}\}\} + a \frac{1-\alpha}{2} n \cdot [\tilde{u}], \quad 0 \leq \alpha \leq 1.$$

If $\alpha = 1$ the numerical flux is called central flux being the average of two solutions. The case $\alpha = 0$, corresponds to the upwind flux which takes into account the direction of the flux.

Figure 2 shows the computed solution of equation (3), considering $a = 2$, $u_0(x) = \sin(\pi x)$, at time $t = 0.1$,

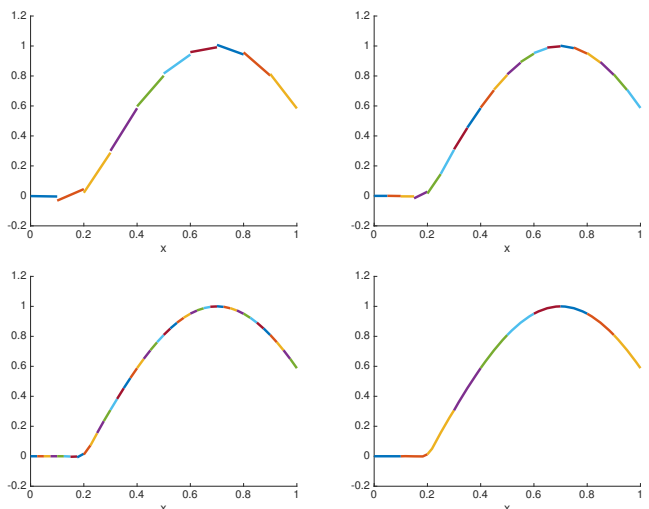


Fig. 2. Numerical solution of the wave equation. Top left: $N = 1, K = 10$. Top right: $N = 1, K = 20$. Bottom left: $N = 1, K = 40$. Bottom right: $N = 4, K = 10$.

obtained by means of the DG method with upwind flux, for different values of N and K .

The flexibility of DG methods allows us to easily change basis functions. For instance, we could use Lagrange polynomials or other polynomials satisfying a desired orthogonality property. One possible choice is to consider the orthonormal basis

$$\varphi_j(r) = \frac{P_j(r)}{\sqrt{\gamma_j}},$$

where P_j are the Legendre polynomials of order j and $\gamma_j = \frac{2}{2j+1}$. This basis can be computed through the recurrence

$$a_{j+1} \varphi_{j+1}(r) = r \varphi_j(r) - a_j \varphi_{j-1}(r),$$

$$a_j = \sqrt{\frac{j^2}{(2j+1)(2j-1)}},$$

with $\varphi_0(r) = \frac{1}{\sqrt{2}}$, $\varphi_1(r) = \sqrt{\frac{3}{2}} r$. The affine mapping

$$x(r) = x_k^l + \frac{1+r}{2} (x_k^r - x_k^l),$$

relates $x \in D_k$ with the reference variable $r \in [-1, 1]$.

We now go back to the more general problem (1) in two or three space dimensions. We will present the discrete setting in both time and space based on DG in time-space discretizations. We will also present a result for the error analysis.

4 Semi-discretization in time

We start by decomposing the time interval $I = (0, T]$ into disjoint subintervals $I_n = (t_{n-1}, t_n]$, where $n = 1, \dots, N$, $0 = t_0 < t_1 < \dots < t_{N-1} < t_N = T$. We use the notation $\tau_n = t_n - t_{n-1}$.

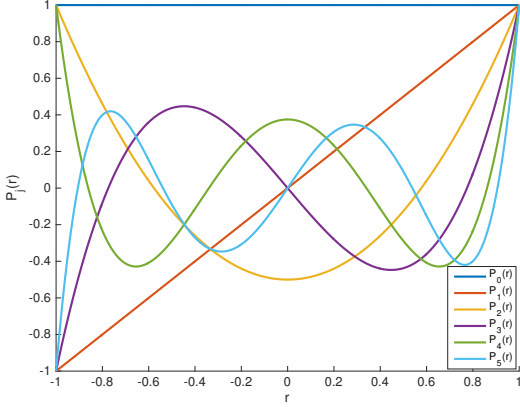


Fig. 3. Legendre polynomials.

The approximate solution is a piecewise polynomial with respect to time, locally defined on the space

$$P_k(I_n, V) = \{w : I_n \rightarrow V, w(t) = \sum_{j=0}^k W^j t^j, \forall t \in I_n, W^j \in V, \quad \forall j\}.$$

The space $P_k(I_n, L^2(\Omega))$ is defined analogously, with V replaced by $L^2(\Omega)$. The jump of w_τ at t_n is defined as

$$[w_\tau]_n = w_\tau(t_n^+) - w_\tau(t_n),$$

where $w_\tau(t_n^+) = \lim_{t \rightarrow t_n^+} w_\tau(t)$. Using the known value $u_\tau(t_{n-1})$ from the previous time interval and u_0 for $n = 1$, the local problem on I_n reads: find $u_\tau|_{I_n} \in P_k(I_n, V)$ such that

$$\begin{aligned} & \int_{I_n} \left(\frac{\partial u_\tau}{\partial t} + Au_\tau, v_\tau \right)_{L^2(\Omega)} dt + ([u_\tau]_{n-1}, v_\tau(t_{n-1}^+))_{L^2(\Omega)} \\ & = Q_n((f, v_\tau)_{L^2(\Omega)}), \end{aligned}$$

$\forall v_\tau \in P_k(I_n, L^2(\Omega))$. The right-hand side is evaluated by means of some numerical integration formula

$$Q_n((f, v_\tau)_{L^2(\Omega)}) \simeq \int_{I_n} (f, v_\tau)_{L^2(\Omega)} dt.$$

5 Space discretization

Let \mathcal{T}_h be a shape-regular mesh of Ω which is assumed to have a polygonal ($d = 2$) or polyhedral ($d = 3$) boundary. By h we denote the mesh diameter. Let V_h be the space of piecewise polynomials of order less or equal to r . The mesh edges or faces (cases $d = 2$ and $d = 3$, respectively) are collected in the set \mathcal{F}_h , split into the set of the ones belonging to the interior, \mathcal{F}_h^{int} , and boundary, \mathcal{F}_h^{ext} .

The discrete operator which defines the DG method in time, A_h , defined for all $v \in H^1(\Omega) \cup V_h$ and $w_h \in V_h$,

is given by

$$\begin{aligned} (A_h v, w_h)_{L^2(\Omega)} &= \sum_{T \in \mathcal{T}_h} (\sigma v + \beta \cdot \nabla v, w_h)_{L^2(T)} \\ &+ \sum_{F \in \mathcal{F}_h^{ext, inflow}} ((\beta \cdot n)v, w_h)_{L^2(F)} \\ &- \sum_{F \in \mathcal{F}_h^{int}} ((\beta \cdot n)[v], \llbracket w_h \rrbracket)_{L^2(F)} \\ &+ \sum_{F \in \mathcal{F}_h^{int}} \left(\frac{1}{2} |\beta \cdot n| [v], [w_h] \right)_{L^2(F)}. \end{aligned}$$

This operator verifies the following important properties.

- Consistency: Let $P_h : L^2(\Omega) \rightarrow V_h$ be the L^2 -orthogonal projector onto V_h . Then

$$A_h w = P_h A w, \quad \forall w \in H^1(\Omega).$$

- Discrete coercivity: Let us consider the mesh-dependent norm

$$\begin{aligned} \|v_h\|^2 &= \mu_0 \|v\|_{L^2(\Omega)}^2 + \sum_{F \in \mathcal{F}_h^{ext}} \| |\beta \cdot n|^{1/2} v \|_{L^2(F)}^2 \\ &+ \frac{1}{2} \sum_{F \in \mathcal{F}_h^{int}} \| |\beta \cdot n|^{1/2} [v] \|_{L^2(F)}^2. \end{aligned}$$

Then $\exists C > 0$ such that

$$C \|v_h\|^2 \leq (A_h v_h, v_h)_{L^2(\Omega)},$$

$\forall v_h \in V_h$.

6 Full space-time discretization

Putting all together, we now derive the fully discrete method.

We consider the finite element space V_h^n resulting from the mesh \mathcal{T}_h^n which can change from one time interval to the next. The local problem in I_n reads: find $u_{\tau h}|_{I_n} \in P_k(I_n, V_h^n)$ such that, for all $v_{\tau h} \in P_k(I_n, V_h^n)$,

$$\begin{aligned} & \int_{I_n} \left(\frac{\partial u_{\tau h}}{\partial t} + A_h u_{\tau h}, v_{\tau h} \right)_{L^2(\Omega)} dt \\ & + ([u_{\tau h}]_{n-1}, v_{\tau h}(t_{n-1}^+))_{L^2(\Omega)} \\ & = Q_n((f, v_{\tau h})_{L^2(\Omega)}). \end{aligned}$$

This method, which was analysed in [7], is unconditionally stable and convergent. The error bound in the following result shows that the method is of arbitrary high order in time and in space.

Theorem 1. *Let u be the exact solution of (2), which is assumed to be enough regular, and let $u_{\tau h}$ be the fully discrete solution of the DG method. Assume that $k \geq 1$ and $\tau_n \leq 1$, for all $n = 1, \dots, N$. Then the following error bound holds for all $m = 1, \dots, N$,*

$$\begin{aligned} & \|u(t_m) - u_{\tau h}(t_m)\|_{L^2(\Omega)} \leq \\ & C \left((E_0)^2 + t_m \max_{1 \leq n \leq m} \left\{ C_n^T(u) \tau_n^{2(k+2)} + C_n^S(u) h^{2r+1} \right\} \right. \\ & \left. + C_m'(u) h^{2(r+1)} \right), \end{aligned}$$

with $C_n^T(u) = |u|_{C^{k+3}(\bar{I}_n, L^2(\Omega))}^2 + |u|_{C^{k+2}(\bar{I}_n, V)}^2$, $C_n^S(u) = \|u\|_{C^1(\bar{I}_n, H^{r+1}(\Omega))}^2$ and $C_m^U(u) = |u(t_m)|_{H^{r+1}(\Omega)}^2$.

The error bound point out not only the influence of the mesh size but also the dependence on the choice of the degree of the polynomials used in the construction of the finite element space, making possible to balance accuracy and computational efficiency.

7 Outlook

The demand for modelling intricate systems often involving multiscales and multiphysics around complex geometries has been a source of motivation for great progress in the field of computational mathematics. High order methods for solving partial differential equations, such as finite element methods or spectral methods, are attractive due to the need of great accuracy on realistic models. Nevertheless a number of challenges still exist not only in the development of new mathematical tools but also in translating academic progresses into engineering practice.

There is a truly need of a formulation and analysis of new multiscale, multiphysics, scalable, parallel efficient methods for treating multiple time and spatial scales that arise in modelling complex phenomena. The arising of new methods demands developments in their analysis and investigators are engaged to seek results on the well-posedness of the models, *a priori* and *a posteriori* error estimators, stability and convergence aspects. Another important issue to address is reliability of computer predictions due to uncertainty. Physical phenomena can rarely be modelled with complete fidelity even under the best of circumstances, even though they often support life-and-death decisions in different fields. The uncertainty may occur in all phases of the predictive process, from model selection and choice of the parameters to the observation data. Mathematicians are driven forward to investigate uncertainty quantification and error estimators.

In the particular topic of the present article, there are still important questions to be addressed. First, the investigation of the theoretical aspects of the DG time-stepping method, as the convergence properties, is far from being closed. The existent literature does not encompasses all models. The introduction of nonlinearities or the change of the boundary conditions, often needed to model real applications, entail subtleties and often the analysis is not straightforward from the existent results. Another challenge appears when applying the DG time-stepping method in practice and we are faced with the task of solving big linear systems at each time-step possible defined by matrixes with large condition numbers. The drawback in the computational cost can be tamed using efficient solvers. There has been a great interest in investigating strategies like multigrid methods, domain decomposition methods and to develop robust and efficient preconditioners. An additional aspect which deserves attention is how to deal efficiently with

the quadrature rules, which involve sums on the quadrature points, in the case of high order methods.

Acknowledgments

This work was partially supported by the Centre for Mathematics of the University of Coimbra – UID/MAT/00324/2013, funded by the Portuguese Government through FCT/MCTES and co-funded by the European Regional Development Fund through the Partnership Agreement PT2020, and by Fundação para a Ciência e a Tecnologia, I.P. through the grant SFRH/BSAB/113774/2015.

References

1. A. Araújo, S. Barbeiro and M. K. Ghalati (2016). Stability of a leap-frog discontinuous Galerkin method for time-domain Maxwell's equations in anisotropic materials, arXiv:1607.06425, to appear in Communications in Computational Physics.
2. A. Araújo, S. Barbeiro and M. K. Ghalati (2016). Convergence of a leap-frog discontinuous Galerkin method for time-domain Maxwell's equations in anisotropic materials, to appear in Progress in Industrial Mathematics at ECMI 2016, Springer, ECMI book subseries of Mathematics in Industry.
3. E. Burman, A. Ern and M. A. Fernandez (2010). Explicit Runge-Kutta Schemes and Finite Elements with Symmetric Stabilization for First-Order Linear PDE Systems, SIAM Journal on Numerical Analysis, 48(6), 2019-2042.
4. G. Chavent and B. Cockburn (1989). The local projection $P^0 - P^1$ -discontinuous-Galerkin finite element method for scalar conservation laws, ESAIM: Mathematical Modelling and Numerical Analysis - Modélisation Mathématique et Analyse Numérique, 23.4: 565-592.
5. B. Cockburn, M. Luskin, C.W. Shu and E. Süli (2003). Enhanced accuracy by post-processing for finite element methods for hyperbolic equations, Mathematics of Computation, 72(2): 577-606.
6. S. Descombes, S. Lanteri and L. Moya (2013). Locally implicit time integration strategies in a discontinuous Galerkin method for Maxwell's equations, Journal of Scientific Computing, 56: 190-218.
7. A. Ern and F. Schieweck (2016). Discontinuous Galerkin method in time combined with a stabilized finite element method in space for linear first-order PDEs, Mathematics of Computation, 85: 2099-2129.
8. L. Fezoui, S. Lanteri, S. Lohrengel and S. Piperno (2005). Convergence and stability of a discontinuous Galerkin time-domain method for the 3D heterogeneous Maxwell's equations on unstructured meshes. ESAIM: Mathematical Modeling and Numerical Analysis, 39(6):1149-1176.
9. M. J. Grote, M. Mehlh and T. Mitkova (2015). Runge-Kutta Based Explicit Local Time-Stepping Methods for Wave Propagation, SIAM Journal on Scientific Computing, 37(2): A747-A775.
10. J. Hesthaven and T. Warburton (2008). Nodal Discontinuous Galerkin Methods: Algorithms, Analysis, and Applications. Springer-Verlag, New York.
11. P. Houston and E. Süli (2001). hp-Adaptive discontinuous Galerkin finite element methods for first-order hyperbolic problems, SIAM Journal on Scientific Computing, 23(4):1225-1251.

12. C. Johnson and J. Pitkäranta (1986). An analysis of the discontinuous Galerkin method for a scalar hyperbolic equation, *Mathematics of Computation*, 46: 1-26.
13. P. Lesaint and P.-A. Raviart (1974). On a finite element method for solving the neutron transport equation, *Mathematical Aspects of Finite Elements in Partial Differential Equations*, 33: 89-123.
14. Q. Lin and A. H. Zhou (1993). Convergence of the discontinuous Galerkin methods for a scalar hyperbolic equation, *Acta Mathematica Scientia*, 13: 207-210.
15. T. E. Peterson (1991). A Note on the Convergence of the Discontinuous Galerkin Method for a Scalar Hyperbolic Equation, *SIAM Journal on Numerical Analysis*, 28(1): 133-140.
16. W. H. Reed and T. Hill (1973). Triangular mesh methods for the neutron transport equation. Los Alamos Report LA-UR-73-479.
17. B. Rivière and M.F. Wheeler (2002). Discontinuous Galerkin methods for flow and transport problems in porous media, *Communications in Numerical Methods in Engineering*, 18: 63-68.
18. M. Santos, A. Araújo, S. Barbeiro, F. Caramelo, A. Correia, M.I. Marques, L. Pinto, P. Serranho, R. Bernardes and M. Morgado (2015). Simulation of cellular changes on optical coherence tomography of human retina. In 2015 37th Annual International Conference of the IEEE Engineering in Medicine and Biology Society (EMBC), 8147-8150.
19. K. Yosida 1995. *Functional analysis, Classics in Mathematics*, Springer-Verlag, Berlin, 1995.